

ments of the stopping cross sections of solids at low energies.

V. ACKNOWLEDGMENTS

The author is indebted to the University of Nebraska Research Council for a Summer Fellowship Grant and

to the University of Illinois Cyclotron Laboratory for the loan of the crystal chamber. Mr. C. E. Kuyatt and Mr. D. C. Lorents helped greatly in the experimental work. It is a very real pleasure to acknowledge the helpful discussions of this problem with Dr. F. S. Eby, Dr. W. K. Jentschke, and Dr. W. G. Cross.

Ferromagnetic Resonance in Two Nickel-Iron Ferrites

W. A. YAGER, J. K. GALT, AND F. R. MERRITT
Bell Telephone Laboratories, Murray Hill, New Jersey

(Received April 19, 1955)

Ferromagnetic resonance data are presented as a function of temperature from 4.2°K to 380°K in $(\text{NiO})_{0.95}(\text{FeO})_{0.05}\text{Fe}_2\text{O}_3$ and in $(\text{NiO})_{0.75}(\text{FeO})_{0.25}\text{Fe}_2\text{O}_3$. When the effects of eddy currents are corrected for, most of the energy dissipation in $(\text{NiO})_{0.75}(\text{FeO})_{0.25}\text{Fe}_2\text{O}_3$ as measured by the resonance line width is shown to be due to a relaxation mechanism associated with the presence of divalent iron. The line width shows a maximum at 160°K at our frequency of measurement (24 000 Mc/sec). A thermodynamical analysis of the loss mechanism is presented which assumes that a torque associated with part of the free energy relaxes. This correlates the line width quite satisfactorily with the temperature dependence observed in the magneto-crystalline anisotropy and the spectroscopic splitting (g) factor.

I. INTRODUCTION

IN recent years, several studies of ferromagnetic resonance line width have been made in single crystals of ferrites.¹⁻⁵ It has, however, remained difficult to understand the mechanism of the losses in these materials. The purpose of the present paper is to report ferromagnetic resonance experiments on single crystals of two ferrite compositions which we feel throw some light on this mechanism. Quantitative chemical analysis for Ni and Fe together with the usual valences give $(\text{NiO})_{0.95}(\text{FeO})_{0.05}\text{Fe}_2\text{O}_3$ and $(\text{NiO})_{0.75}(\text{FeO})_{0.25}\text{Fe}_2\text{O}_3$ as the simplest formulas for the compositions on which we have worked. There is some possibility of small variations from these formulas in detail, but they are at least good approximations. The first of these compositions was grown by J. P. Remeika at Bell Laboratories using a slight variation on a method previously reported⁶ which involves solutions of the constituent oxides in borax at high temperatures. The second composition was grown by Dr. G. W. Clark of the Linde Air Products Company by means of a flame fusion method.

Our data consist of: (1) resonant field as a function of crystal orientation, and (2) the width of the resonance line for both ferrites as a function of temperature from 4.2° to 380°K and as a function of crystal direction at several temperatures. Because they showed features of special interest, preliminary data on line width as a function of temperature in $(\text{NiO})_{0.75}(\text{FeO})_{0.25}\text{Fe}_2\text{O}_3$ have been reported previously.⁷

From our data we are able to deduce for each temperature the magnetocrystalline anisotropy constants K_1 and K_2 , the general damping parameter λ , and the spectroscopic splitting factor g . The analysis used to deduce these parameters is simple and has been presented elsewhere.^{1,2,8} We will therefore merely summarize results which we must use. The technique of this experiment will also be discussed only briefly, since it is very similar to previous work done by us on small oriented spheres in a microwave cavity.^{2,3}

We present in more detail an elementary thermodynamical theory of the line-width data in terms of the idea that a large part of the losses in ferrites arise from relaxations associated with electronic rearrangements like that which occurs in the low-temperature transition in Fe_3O_4 . We suggest that the maximum in the line width at 160°K which we see in the data on $(\text{NiO})_{0.75}(\text{FeO})_{0.25}\text{Fe}_2\text{O}_3$ (see Fig. 3) is due to such a relaxation associated with a rearrangement of the valence electrons on the iron ions as the magnetization moves. The suggestion that motion of these valence electrons is involved in losses has been made before by

¹ L. R. Bickford, Jr., Phys. Rev. **78**, 449 (1950). Technical Report XXIII Laboratory for Insulation Research Massachusetts Institute of Technology October, 1949 (unpublished).

² Yager, Galt, Merritt, and Wood, Phys. Rev. **80**, 744 (1950).

³ Galt, Yager, Remeika, and Merritt, Phys. Rev. **81**, 470 (1951).

⁴ D. W. Healy, Jr., Phys. Rev. **86**, 1009 (1952).

⁵ T. Okamura and Y. Kojima, Phys. Rev. **86**, 1040 (1952); T. Okamura, Sci. Rept. Research Inst. Tôhoku Univ. **A6**, 89 (1954).

⁶ Galt, Matthias, and Remeika, Phys. Rev. **78**, 391 (1949). Remeika grew the $(\text{NiO})_{0.95}(\text{FeO})_{0.05}\text{Fe}_2\text{O}_3$ used in the present experiments with sodium metaborate as a flux, rather than the sodium tetraborate used in this reference.

⁷ Galt, Yager, and Merritt, Phys. Rev. **93**, 1119 (1954).

⁸ C. Kittel, Phys. Rev. **73**, 155 (1948).

Wijn and van der Heide for other ferrites at other frequencies.⁹

In terms of this theory of the line width, we are able to relate our results to the results of measurements of the viscous damping of an individual ferromagnetic domain wall as a function of temperature in $(\text{NiO})_{0.75}(\text{FeO})_{0.25}\text{Fe}_2\text{O}_3$. Such measurements have recently been made by one of us and discussed in these same terms.¹⁰

II. EXPERIMENTAL

The experimental technique was fundamentally the same as that previously described.² We will therefore only discuss those aspects of the later experiments which were different.

The most important changes were those required in order to reach low temperatures. The transmission-type cavity was at the end of a vertical run of the input and output wave guides which extended for some three feet. Of this vertical run about eight inches consisted of rectangular glass tubing of the same inside dimensions as the rest of the wave guide, with the inside walls silver plated to provide the necessary electrically conducting surfaces. The glass tubing abutted against suitable joints with the wave guide at each end, and the assembly was held together by wires which applied a compressive stress between the two sets of joints. This arrangement cut the heat leak down to quite acceptable values.

The cavity was placed inside a helium Dewar. The space between the sidewalls of this Dewar was connected through a stopcock to a pump lead so that a pressure of about 2 mm of N_2 gas at room temperature could be established in it before each run. When this Dewar contained liquid He, the N_2 condensed on the outside of the inner wall and minimized the diffusion of He through the glass. The Dewar extended well up above the glass sections in the wave guides. This helium Dewar, in turn, was inside another Dewar which could be filled with liquid nitrogen. A vacuum pump was connected to this Dewar assembly in such a way that it was possible to pump on the liquid helium.

These experiments were done with an electromagnet built by A. D. Little Company which could be rotated about a vertical axis. This made an important innovation possible in the measurement of magnetocrystalline anisotropy. The spherical single crystal of ferrite was mounted in the cavity in a fixed position with the (110) plane parallel to both the dc and the rf magnetic fields. The field required for resonance was observed as a function of crystal direction by rotating the electromagnet, not by rotating the crystal. This especially simplified the experiments at low temperatures.

The values of the applied magnetic field were meas-

ured by means of proton or lithium nuclear resonance as in previous work.²

The spherical samples were made with a device developed for the purpose by Bond.¹¹

The cavity used in these experiments could not be tuned. Rather, the signal oscillator was tuned to the resonant frequency of the cavity. For this reason, line widths were measured with a method somewhat different from that used in reference 2. A sphere was placed loose in a polystyrene cup in the cavity, so that the dc field oriented it with a [111] direction parallel to the field. Then the field was rotated until it was so far from perpendicular to the rf field that the resonance line was quite weak; as a result the sample did not change the frequency of the cavity or the signal transmitted through significantly, even at resonance. Under these conditions, the dc magnetic field was modulated at 280 cps and the resulting *variation* in the transmitted signal was observed. If the conditions are as stated, this variation is proportional to the *slope* of the resonance absorption line [see Eqs. (6) and (16) in reference 2]. What we did experimentally, then, was to measure the separation in oersteds of the points of maximum slope on the resonance lines in this way. This has been converted to the corresponding Lorentzian line width at half-power points before plotting it in Figs. 3, 4, and 5. This technique could only be used with the dc magnetic field along a [111] crystal direction of course. When the field was along other crystal directions, line width data were taken with a sample fixed on a mounting rod. In these cases, the dc field was made to be far from perpendicular to the rf field by adjusting the rotational position of the mounting rod. The method was the same in all other respects.

III. ANALYSIS

Kittel⁸ has derived the resonance condition taking account of sample shape, crystal anisotropy, and the spectroscopic splitting factor. He gives

$$\omega = \gamma H_{\text{eff}}, \quad (1)$$

where ω is the frequency in radians/sec, γ is the gyromagnetic ratio ($ge/2mc$), g is the spectroscopic splitting factor, and

$$H_{\text{eff}} = \{ [H_z + (N_y + N_y^e - N_z)M_z] \\ \times [H_z + (N_x + N_x^e - N_z)M_z] \}. \quad (2)$$

Here N_x , N_y , and N_z are the usual shape demagnetizing factors and N_x^e , N_y^e are effective demagnetizing factors which are a convenient way of taking account of the crystalline anisotropy. In our experiments with spheres $N_x = N_y = N_z$, so these factors cancel out, and Eq. (2) becomes

$$H_{\text{eff}} = [(H_z + N_y^e M_z)(H_z + N_x^e M_z)]^{\frac{1}{2}}. \quad (3)$$

Since $N_y^e M_z$ and $N_x^e M_z$ turn out experimentally to be

¹¹ W. L. Bond, Rev. Sci. Instr. 22, 344 (1951).

⁹ H. P. J. Wijn and H. van der Heide, Revs. Modern Phys. 25, 98 (1953). H. P. J. Wijn, thesis, Leiden, 1953 (unpublished). Separaat 2092, N.V. Philips Gloeilampenfabrieken, Eindhoven, Holland.

¹⁰ J. K. Galt, Bell System Tech. J. 33, 1023 (1954).

at all times less than 10% of H_z at 24 000 Mc/sec, we may write:

$$H_{\text{eff}} = H_z + \frac{1}{2}(N_y^e + N_x^e)M_z. \quad (4)$$

N_y^e and N_x^e are, of course, functions of crystal direction. They include terms in both K_1 and K_2 and we may therefore write:

$$H_{\text{eff}} = H_z + f_1(\theta)K_1/M_z + f_2(\theta)K_2/M_z, \quad (5)$$

where θ is the angle of rotation in a crystal plane. If we let θ be the angle in the (110) plane between H_z and the [100] direction, Bickford¹ has shown that

$$\begin{aligned} f_1(\theta) &= 2 - (5/2)\sin^2\theta - (15/8)\sin^22\theta, \\ f_2(\theta) &= \frac{1}{4}(\sin^4\theta - 4\sin^22\theta + 4\cos^4\theta)\sin^2\theta. \end{aligned} \quad (6)$$

Equations (5) and (6) were used in conjunction with the measured values of H_z as a function of θ to determine H_{eff} , K_1/M_z , and K_2/M_z at each temperature of measurement. In most cases a least squares procedure was used to fit Eq. (5) to the experimental data.

The value of H_{eff} obtained from Eqs. (5) and (6) at each temperature is used in Eq. (1) to determine the g value for that temperature. The values of K_1 and K_2 are obtained from K_1/M_z and K_2/M_z by assuming that M_z is the saturation magnetization of the ferrite at the temperature of measurement.

Since our most accurate line width measurement is of the separation between points of maximum slope on the absorption line rather than between half-power points, we convert our data to the width of the corresponding Lorentzian line at half-power points. This is done by means of the following relation:

$$(2\Delta H)_{\text{max slope}} = (1/\sqrt{3})(2\Delta H)_{\text{half-power}}, \quad (7)$$

where $(2\Delta H)$ is the total width of the line in each case. All line widths presented in the present paper are $(2\Delta H)_{\text{half-power}}$.

It is convenient to derive the damping constant λ from the line width, since it is a more general parameter

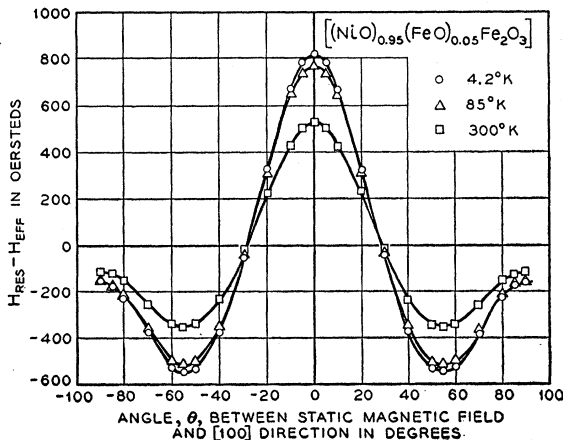


FIG. 1. $(H_{\text{res}} - H_{\text{eff}})$ as a function of angle between \mathbf{M} and [100] direction in (110) plane for $(\text{NiO})_{0.95}(\text{FeO})_{0.05}\text{Fe}_2\text{O}_3$.

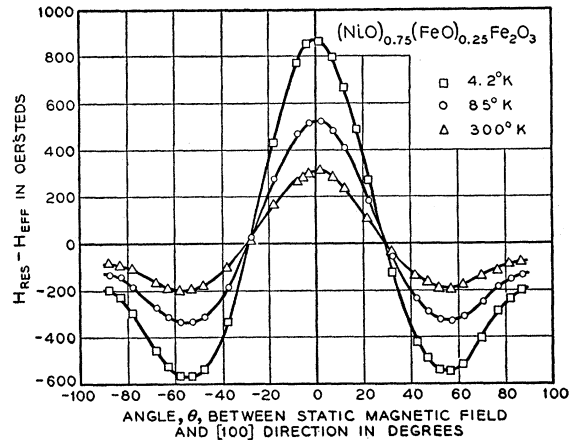


FIG. 2. $(H_{\text{res}} - H_{\text{eff}})$ as a function of angle between \mathbf{M} and [100] direction in (110) plane for $(\text{NiO})_{0.75}(\text{FeO})_{0.25}\text{Fe}_2\text{O}_3$.

with which to characterize the losses. λ is defined by writing for the equation of motion \mathbf{M} :

$$d\mathbf{M}/dt = \gamma[\mathbf{M} \times \mathbf{H}] - (\lambda/M^2)[\dot{\mathbf{M}} \times (\dot{\mathbf{M}} \times \mathbf{H})]. \quad (8)$$

A relation between λ and the line width is given by Eq. (A-6) in reference 2. The relation given there is slightly incorrect, however.¹² It should be

$$(2\Delta H)_{\text{half-power}}/H_{\text{eff}} = 2\lambda/\gamma M_z. \quad (9)$$

Note that if $(2\Delta H)$ is independent of crystal direction, Eq. (9) shows that λ is too. The α in reference 2 is equal to $\lambda/\gamma M_z$ in the notation of the present paper.

IV. RESULTS

Figures 1 and 2 show how the applied field required for resonance varies with crystal direction in the (110) plane for $(\text{NiO})_{0.95}(\text{FeO})_{0.05}\text{Fe}_2\text{O}_3$ and $(\text{NiO})_{0.75}(\text{FeO})_{0.25}\text{Fe}_2\text{O}_3$, respectively.

It will be seen that our anisotropy results at 77°K for $(\text{NiO})_{0.95}(\text{FeO})_{0.05}\text{Fe}_2\text{O}_3$ differ substantially from those obtained by Healy on NiOFe_2O_3 .⁴ The differences are largest near the [100] direction. It seems doubtful that this disagreement can be accounted for by the deviation of the composition of our crystals from NiOFe_2O_3 , since Healy's crystals came from the same source, and there is every reason to believe that they deviated from NiOFe_2O_3 in the same way. It should be noted that our data confirm the variation of K_1 with temperature as measured previously by a simpler but less accurate method at 60 cycles on stoichiometric NiOFe_2O_3 .⁶ We do not at present have a satisfactory explanation for this discrepancy.

Table I gives K_1/M , K_2/M , M , K_1 , K_2 , H_{eff} , ν , g , and λ for $(\text{NiO})_{0.95}(\text{FeO})_{0.05}\text{Fe}_2\text{O}_3$. Table II gives the same data for $(\text{NiO})_{0.75}(\text{FeO})_{0.25}\text{Fe}_2\text{O}_3$. Note that the values of K_1 in Table II are somewhat different from

¹² Equation (A-6) in reference 2 fails to take proper account of the dependence of l_z and l_y on H_z . This error occurs in reference 10 also.

TABLE I. $(\text{NiO})_{0.95}(\text{FeO})_{0.05}\text{Fe}_2\text{O}_3$.

$T^\circ\text{K}$	K_1/M	K_2/M	M (cgs units)	K_1 (ergs/cc)	K_2 (ergs/cc)	H_{eff} (oe)	ν (Mc/sec)	g (cgs units)	λ (H parallel to [111] dir.) (cgs units) (corrected for eddy currents)
298	-254	-70 \pm 50	270	-68 \times 10 ³	(-19 \pm 13) \times 10 ³	7917	24 338	2.196	2.9 \times 10 ⁷
85	-370	-100 \pm 50	290	-107 \times 10 ³	(-29 \pm 14) \times 10 ³	7942	24 450	2.198	3.7 \times 10 ⁷
4.2	-392	-120 \pm 50	300	-118 \times 10 ³	(-36 \pm 15) \times 10 ³	7743	23 880	2.202	2.2 \times 10 ⁷

TABLE II. $(\text{NiO})_{0.75}(\text{FeO})_{0.25}\text{Fe}_2\text{O}_3$.

$T^\circ\text{K}$	K_1/M	K_2/M	M (cgs units)	K_1 (ergs/cc)	K_2 (ergs/cc)	H_{eff} (oe)	ν (Mc/sec)	g (cgs units)	λ (H parallel to [111] dir.) (cgs units) (corrected for eddy currents)
300	-152	+16	322	-49 \times 10 ³	+5.2 \times 10 ³	8195	24 388	2.13	10 \times 10 ⁷
159	-218	+3	338	-74 \times 10 ³	+1.0 \times 10 ³	8094	24 461	2.16	14 \times 10 ⁷
135	-238	+14	339	-81 \times 10 ³	+4.7 \times 10 ³	8054			14 \times 10 ⁷
85	-259	+24	340	-88 \times 10 ³	+8.2 \times 10 ³	7980	24 471	2.19	10 \times 10 ⁷
4.2	-421	-15	342	-144 \times 10 ³	-5.1 \times 10 ³	7901	23 946	2.16	3 \times 10 ⁷

the preliminary data given in reference 10. The present data are the more accurate. Note also from Table II that the g factor in these single crystals is temperature dependent. This is not the case for $(\text{NiO})_{0.95}(\text{FeO})_{0.05}\text{Fe}_2\text{O}_3$. This variation in g factor cannot be explained as a size effect; no such variation occurs in the value of the resonance field in the [111] direction, for example, among the 6, 7, and 9 mil spheres at any of the temperatures at which we took data.

The magnetizations of the $(\text{NiO})_{0.95}(\text{FeO})_{0.05}\text{Fe}_2\text{O}_3$ in Table I are obtained from Healy's⁴ data and from measurements made in these Laboratories. The values of M_s for $(\text{NiO})_{0.75}(\text{FeO})_{0.25}\text{Fe}_2\text{O}_3$ in Table II are those used in connection with the domain wall studies on the same material made by one of us.¹⁰ In this case the room temperature value is measured, and the values at other temperatures are determined from the assumption

that M_s varies with temperature in this material in the same way as it does in Fe_3O_4 as measured by Weiss and Forrer.¹³

Figure 3 shows the line widths at each temperature for both compositions when the dc magnetic field is along the [111] direction. The values are plotted in the high temperature region for several sample sizes of the $(\text{NiO})_{0.75}(\text{FeO})_{0.25}\text{Fe}_2\text{O}_3$ composition. We believe that the rise in line width in this composition at these temperatures is due to the loss arising from the increasing conductivity of these crystals. This is confirmed by the fact that the size dependence in the line width characteristic of the relatively high conductivity ferrites¹⁴ is observed in this region, and by the fact that crystals of the sort from which these spheres are cut have resistivities of only about 1 ohm-cm at room temperature.¹⁵ The high-temperature end of the $(\text{NiO})_{0.75}(\text{FeO})_{0.25}\text{Fe}_2\text{O}_3$ curves may therefore be understood at least qualitatively in terms of a loss mechanism (eddy currents) which is not new and not of primary importance in understanding the losses in ferrites generally.

The low-temperature portion of these curves, however, is quite another matter. The bulk of the loss in this region is clearly due to a mechanism whose effectiveness is a maximum in the neighborhood of 160 $^\circ\text{K}$. Furthermore this mechanism clearly has something to do with the presence of divalent iron in the ferrite, since it has almost disappeared in the $(\text{NiO})_{0.95}(\text{FeO})_{0.05}\text{Fe}_2\text{O}_3$ composition. Figure 4 shows plots of the line width in $(\text{NiO})_{0.75}(\text{FeO})_{0.25}\text{Fe}_2\text{O}_3$ as a function of temperature for various directions of the dc magnetic field. Figure 5 shows a continuous plot of the line width as a function of direction in the (110) plane at 85 $^\circ\text{K}$. Clearly this loss mechanism is quite anisotropic.

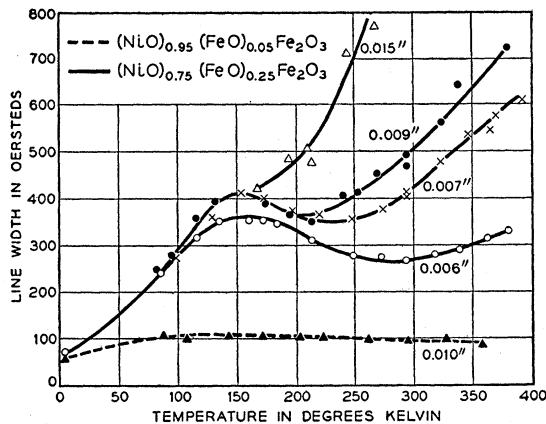


FIG. 3. Ferromagnetic resonance line width as a function of temperature for both ferrite compositions measured with dc magnetic field in [111] crystal direction. Note the size effect at high temperatures in $(\text{NiO})_{0.75}(\text{FeO})_{0.25}\text{Fe}_2\text{O}_3$; this is attributed to conductivity. The line is somewhat distorted in shape when this size effect is larger.

¹³ P. Weiss and R. Forrer, Ann. phys. Series 10, 12, 279 (1929).

¹⁴ Yager, Merritt, and Guillaud, Phys. Rev. 81, 477 (1951).

¹⁵ T. H. Geballe and F. J. Morin (to be published).

The anisotropy in $(2\Delta H)$ for $(\text{NiO})_{0.95}(\text{FeO})_{0.05}\text{Fe}_2\text{O}_3$ is smaller than that for $(\text{NiO})_{0.75}(\text{FeO})_{0.25}\text{Fe}_2\text{O}_3$ as expected from the fact that $(2\Delta H)$ itself is smaller. Our measurements of line width in directions other than $[111]$ for this material, however, are not sufficiently accurate to justify giving numerical values.

The absolute accuracy of the line width measurements gets worse as line intensity increases, for reasons discussed in Sec. II. We have made line intensity measurements which indicate that our relative errors, and our absolute errors in data taken at 85°K and below are 5% or less. The absolute errors in some of the line widths at temperatures above 85°K may be as large as 15%.

V. PHENOMENOLOGICAL THEORY

Having presented our data in the conventional way, we now turn to an elementary thermodynamical theory of the losses which explains at least qualitatively the maximum in the line width in $(\text{NiO})_{0.75}(\text{FeO})_{0.25}\text{Fe}_2\text{O}_3$. As we have seen above, it is fairly clear that this contribution to the losses arises from a relaxation associated with the fact that as the magnetization \mathbf{M} moves the valence electrons on the iron ions are rearranged. The rearrangement does not occur fast enough to keep up with the motion of \mathbf{M} , and as a result a net energy loss occurs.

It is not obvious, however, exactly what it is that relaxes, or to put it another way, what the time dependent interaction between the magnetic lattice and the electrons is. Some of the alternatives have been discussed in connection with the domain wall studies in reference 10. Following reference 10, we shall illustrate the mechanism by carrying out a calculation of the line width on the assumption that the torque on the magnetization associated with part of the free energy relaxes. As we shall see, however, we must assume that this part of the free energy must include another term in addition to the cubic anisotropy energy assumed in

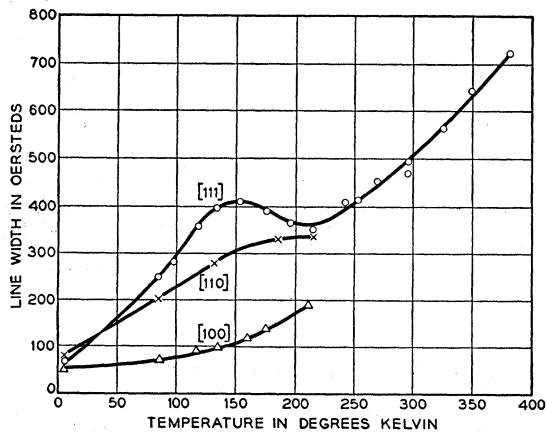


FIG. 4. Ferromagnetic resonance line width in $(\text{NiO})_{0.75}(\text{FeO})_{0.25}\text{Fe}_2\text{O}_3$ as a function of temperature with the dc magnetic field in the three principal crystal directions. These data were obtained from the 0.009-in. sphere.

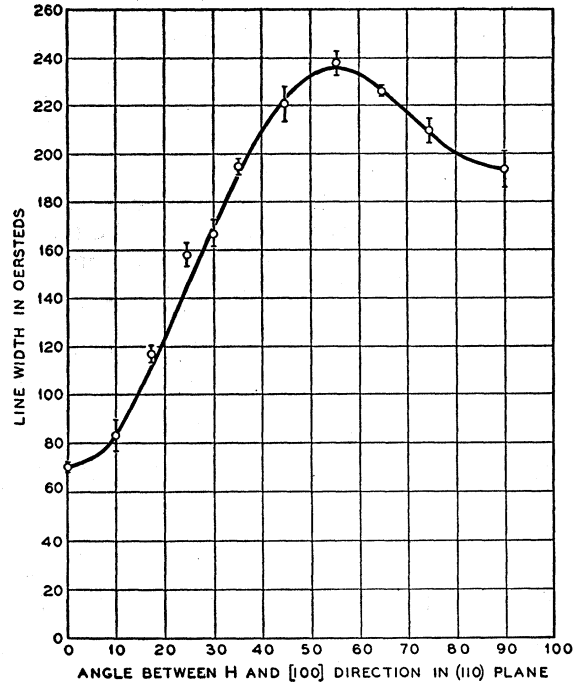


FIG. 5. Ferromagnetic resonance line width in $(\text{NiO})_{0.75}(\text{FeO})_{0.25}\text{Fe}_2\text{O}_3$ as a function of angle between \mathbf{M} and the $[100]$ direction in the (110) plane. These data were taken at 85°K.

reference 10 in order to account for our experimental data on line width.

To proceed, we define our thermodynamical system as the whole magnetic lattice of the sample, which in our present experiments is one saturated magnetic domain. We assume as in reference 10 [Eq. (15)] that

$$\langle dw/dt \rangle_{AV} = \langle dg/dt \rangle_{AV}, \quad (10)$$

where the angular braces denote averages, dw is work done on the system, and dg is a change in the free energy of the system.

In the Appendix, the following expression for the line width at half-power points, $(2\Delta H)$, is derived on the basis of these thermodynamical considerations:

$$2\Delta H = \frac{1}{M_z} \left[\left(\frac{\partial^2 g_{100}}{\partial \theta_x^2} \right)_{\theta_x=0} + \left(\frac{\partial^2 g_{100}}{\partial \theta_y^2} \right)_{\theta_y=0} \right] \frac{\omega \tau}{1 + (\omega \tau)^2}. \quad (11)$$

Here τ is the time associated with the rearrangement of the electrons, and g_{100} is the difference between the anisotropy energy when measured adiabatically (at high frequency compared to $1/\tau$) and when measured isothermally (at low frequency). This g should not be confused with the spectroscopic splitting factor. θ_x and θ_y are the angular deviations of \mathbf{M} from equilibrium. It is clear that much more remains to be done in the theoretical analysis of the effect, but it is nevertheless instructive to compare the line-width data in Figs. 3 and 4 with Eq. (11). This is done in the next section.

Néel^{16,17} has presented an analysis of the dissipation due to the migration of carbon in iron based on a fairly detailed model of the mechanism. Such an analysis might also be applied to our results but this is beyond the scope of the present paper.

VI. DISCUSSION

When we fit Eq. (11) to the line width data in Fig. 3, we first note (primarily from the shape of the $(2\Delta H)$ vs T curve for the $(\text{NiO})_{0.95}(\text{FeO})_{0.05}\text{Fe}_2\text{O}_3$ composition) that the mechanism which gives us our maximum in line width at 160°K does not account for all the losses in these materials. There is an additional contribution for it as follows. We have assumed that in the $(\text{NiO})_{0.95}(\text{FeO})_{0.05}\text{Fe}_2\text{O}_3$ the contribution to $(2\Delta H)$ from the rearrangement of electrons on the iron ions, which gives us the maximum at 160°K, is down from that in $(\text{NiO})_{0.75}(\text{FeO})_{0.25}\text{Fe}_2\text{O}_3$ by about the ratio of the amount of divalent iron in the two cases. We have also assumed that plots of the contribution of this mechanism in the two cases have similar shapes. Such assumptions lead to the result that the unexplained contribution to $(2\Delta H)$ is equal to 40 oersteds in both materials at all temperatures from 85°K up. We have therefore subtracted 40 oersteds from the line-width data given in Fig. 3 for $(\text{NiO})_{0.75}(\text{FeO})_{0.25}\text{Fe}_2\text{O}_3$ before fitting it to Eq. (11).

If we assume $\omega\tau=1$ at the temperature of the maximum in the line width (160°K), we find from the line width (see Fig. 3) at that point and Eq. (11) that $[(\partial^2 g_{100}/\partial\theta_x^2)_{\theta_x=0} + (\partial^2 g_{100}/\partial\theta_y^2)_{\theta_y=0}] = 640M_z$. If we put this back into Eq. (11), and note that $\omega = 1.54 \times 10^{11}$ in these experiments, we find that τ behaves as shown in Fig. 6 as a function of temperature. The accuracy of this plot, especially at 85°K, may be rather poor, but if we fit it to a function of the form,

$$\tau = \tau_\infty e^{\epsilon/kT}, \quad (12)$$

we find from the data in Fig. 6,

$$\epsilon = 0.022 \text{ electron volts, } \tau_\infty = 1.0 \times 10^{-12} \text{ sec.}$$

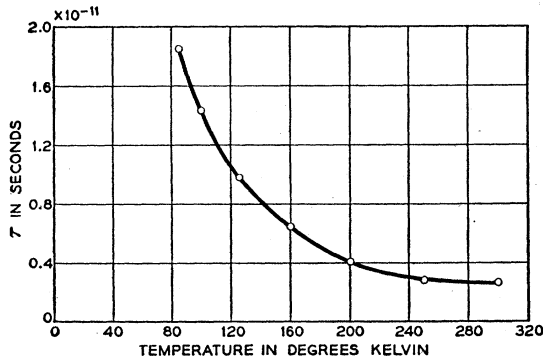


FIG. 6. Relaxation time τ as derived from the data in Figs. 3 and 4 corrected for eddy currents and Eq. (11).

¹⁶ L. Néel, *J. phys. radium* **12**, 339 (1951); **13**, 249 (1952).

¹⁷ J. K. Galt, *Bell System Tech. J.* **34**, 441 (1955).

It will be noted that this value of ϵ is in very good agreement with the activation energy for the production of carriers deduced from measurements of conductivity and thermoelectric power in a very similar ferrite crystal by Geballe and Morin.¹⁵ Bloembergen and Wang¹⁸ have also deduced a relaxation time which increases at low temperatures from ferromagnetic resonance data.

When we try to write an explicit form for g_{100} such that we can account for the line width data in Figs. 3, 4, and 5, we are forced to a more complicated form than previous thinking¹⁰ led us to expect. A form which works is

$$g_{100} = a(\theta_x^2 + \theta_y^2) + K_{1r}(\alpha_1^2\alpha_2^2 + \alpha_2^2\alpha_3^2 + \alpha_3^2\alpha_1^2). \quad (13)$$

The fact that the first term in Eq. (13) is not single valued in the angular position of \mathbf{M} is at first unsettling. However, when we remember that the energy of the magnetization in a magnetic field is of the form $E = -MH(1 + \cos\delta)$, we see that for small deviations δ of \mathbf{M} from \mathbf{H} the second-order term is the important one; it is $\frac{1}{2}MH\delta^2$, which is of the form of the first term in Eq. (13). In other words, this term implies a relaxation in the torque associated with part of the energy of the magnetization in the total effective field. The physical basis of this term is not entirely clear to us, but it leads us to expect a relaxation in the observed g factor. Inspection of Table II shows that our data confirm this expectation qualitatively. Table II also shows between 85°K and room temperature a variation in K_1 of the sort which the second term in Eq. (13) leads us to expect. The further change in K_1 observed between 4.2°K and 85°K must arise from other causes.

Now more quantitatively, if we differentiate Eq. (13), we find

$$\left(\frac{\partial^2 g_{100}}{\partial\theta_x^2}\right)_{\theta_x=0} + \left(\frac{\partial^2 g_{100}}{\partial\theta_y^2}\right)_{\theta_y=0} = 4(a + K_{1r}) - 20K_{1r}\left(\frac{1}{4}\sin^4\theta_0 + \sin^2\theta_0\cos^2\theta_0\right), \quad (14)$$

where θ_0 is the angle between \mathbf{M} and the $[100]$ crystal direction in the (100) plane. If we use Eq. (14) in Eq. (11), we can determine a and K_{1r} from the assumptions that at 160°K $\omega\tau=1$, and that the contributions from this mechanism to $(2\Delta H)$ in the $[100]$ and $[111]$ directions are zero and 320 oersteds respectively. Note that the difference between the $(2\Delta H)$ in the $[100]$ direction at this temperature and the residual 40 oersteds is apparently due to eddy currents. We find for a and K_{1r} :

$$K_{1r} = -32000 \text{ ergs/cc, } a = 32000 \text{ ergs/cc.}$$

These parameters together with the τ at 85°K from Fig. 6 can be used in Eqs. (11) and (14) to fit the $(2\Delta H)$ data in Fig. 5 quite satisfactorily, especially when we remember that the value of τ given in Fig. 6 at 85°K may be in error by 25%. Furthermore the

¹⁸ N. Bloembergen and S. Wang, *Phys. Rev.* **93**, 72 (1954).

data in Table II show that the change in K_1 observed between 300°K and 85°K is minus 39 000 ergs/cc. In view of the possibility that other factors may be causing a change in K_1 over this temperature range, we feel that this is in quite satisfactory *quantitative* agreement with the above value of K_{1r} . The remarks below Eq. (13) suggest that a may be represented by $(MH)_r/2$, so that the torque associated with an MH product of 64 000 ergs/cc is relaxing. This is approximately 2.5% of the value of (MH) for the saturation magnetization in the total effective field. As Table II shows, we observe a 3% change in g factor, which is how such an effect would be observed in our experiments. This also seems like quite satisfactory quantitative agreement, even though the physical basis of the first term in Eq. (13) is not clear.

Clogston¹⁹ has analyzed this mechanism using a theory similar to that of Néel.¹⁶ Because he assumes a much more detailed model than we do, he is able to derive the necessary terms in the free energy, rather than to assume them as is done in Eq. (13).

The λ we find from the present analysis [see Appendix Eq. (A11)] is very different in temperature dependence from that calculated from the domain wall data in reference 10. The difference, however, is easy to understand. It is due to the fact that the domain wall experiments are done in such a way that all angular frequencies associated with the motion are less than $1/\tau$. In that experiment we are therefore restricting ourselves at all temperatures to the region where $\omega\tau \ll 1$. In this case, as we see from Eq. (A11), $\lambda \sim \tau$; it therefore shows an exponential increase at low temperatures. In the present experiment, ω is held constant as a function of temperature, and $\omega\tau$ assumes values above one at low temperatures and below one at high temperatures. We therefore expect from Eq. (A11) a λ which shows a maximum in its variation with temperature, and this is what we observe.

The authors wish to express their gratitude to B. B. Cetlin, H. W. Dail, and M. R. Tiner for technical assistance. Chemical analyses were made by H. E. Johnson, J. F. Jensen, and J. P. Wright. Enlightening discussions were had with A. M. Clogston. Useful comments on the manuscript were made by R. M. Bozorth, J. F. Dillon, S. Geschwind, and S. Millman.

APPENDIX

If we take axes as usual with z along the equilibrium direction of the magnetization, and if we define θ_x as the angular deflection of \mathbf{M} as M_x increases from zero, and θ_y the angular deflection of \mathbf{M} as M_y increases from zero:

$$\begin{aligned} \frac{dg}{dt} &= \frac{\partial g}{\partial \theta_x} \frac{d\theta_x}{dt} + \frac{\partial g}{\partial \theta_y} \frac{d\theta_y}{dt}, \\ &= g_x' \frac{d\theta_x}{dt} + g_y' \frac{d\theta_y}{dt}. \end{aligned} \quad (\text{A1})$$

Since \mathbf{M} is precessing, we have,

$$\begin{aligned} \theta_x &= \theta_{x0} \cos \omega t = (M_{x0}/M_z) \cos \omega t, \\ \theta_y &= \theta_{y0} \cos \omega t = (M_{y0}/M_z) \cos(\omega t - \pi/2), \end{aligned} \quad (\text{A2})$$

and from this of course it is easy to get $d\theta_x/dt$ and $d\theta_y/dt$.

We now calculate g_x' and g_y' . The electrons rearrange to minimize a free energy, so the form we use for g must be such that it is positive. Furthermore, we must form our analysis in such a way that a maximum is established for \mathbf{g}' , since even if the magnetization moves infinitely rapidly, \mathbf{g}' does not become infinite. We therefore write g in the form $g = g_{1\infty} - g_1$, so that $\mathbf{g}' = \mathbf{g}_{1\infty}' - \mathbf{g}_1'$, where \mathbf{g}_1' relaxes toward $\mathbf{g}_{1\infty}'$. Note that the torque relaxes downward from a value $\mathbf{g}_{1\infty}'$, associated with the adiabatic anisotropy energy (fast motions of the magnetization) to a value, zero, associated with the isothermal anisotropy energy (slow motions of the magnetization). We therefore assume that \mathbf{g}_1' relaxes thus:

$$d\mathbf{g}_1'/dt = (\mathbf{g}_{1\infty}' - \mathbf{g}_1')/\tau, \quad (\text{A3})$$

where τ is the time associated with the process of rearranging the electrons. We have for the components of $\mathbf{g}_{1\infty}'$:

$$\begin{aligned} g_{1\infty x}' &= \left(\frac{\partial g_{1\infty}}{\partial \theta_x} \right)_{\theta_x=0} + \left(\frac{\partial^2 g_{1\infty}}{\partial \theta_x^2} \right)_{\theta_x=0} \theta_x, \\ g_{1\infty y}' &= \left(\frac{\partial g_{1\infty}}{\partial \theta_y} \right)_{\theta_y=0} + \left(\frac{\partial^2 g_{1\infty}}{\partial \theta_y^2} \right)_{\theta_y=0} \theta_y. \end{aligned} \quad (\text{A4})$$

The terms in $(\partial g_{1\infty}/\partial \theta_x)$ and $(\partial g_{1\infty}/\partial \theta_y)$ are zero or cancelled by other torques when the magnetization is in equilibrium. It is therefore the terms in $(\partial^2 g_{1\infty}/\partial \theta_x^2)$ and $(\partial^2 g_{1\infty}/\partial \theta_y^2)$ which determine the variations in torque as the magnetization precesses and which are to be used in the component relaxation equations to determine g_{1x}' and g_{1y}' . The solutions are

$$\begin{aligned} g_{1x}' &= \left(\frac{\partial^2 g_{1\infty}}{\partial \theta_x^2} \right)_{\theta_x=0} \frac{\theta_x \cos(\omega t + \varphi)}{[1 + (\omega\tau)^2]^{\frac{1}{2}}}, \\ g_{1y}' &= \left(\frac{\partial^2 g_{1\infty}}{\partial \theta_y^2} \right)_{\theta_y=0} \frac{\theta_y \cos(\omega t + \varphi - \pi/2)}{[1 + (\omega\tau)^2]^{\frac{1}{2}}}, \end{aligned} \quad (\text{A5})$$

where $\tan \varphi = -\omega\tau$. We now have from (A1),

$$\frac{dg}{dt} = (g_{1\infty x}' - g_{1x}') \frac{d\theta_x}{dt} + (g_{1\infty y}' - g_{1y}') \frac{d\theta_y}{dt}. \quad (\text{A6})$$

The terms in $g_{1\infty x}'$ and $g_{1\infty y}'$ give zero when averaged over a cycle. When averaged, we find from A2 and A4,

$$\begin{aligned} \left\langle \frac{dg}{dt} \right\rangle_{\text{av}} &= \frac{1}{2} \left[M_{x0}^2 \left(\frac{\partial^2 g_{1\infty}}{\partial \theta_x^2} \right)_{\theta_x=0} \right. \\ &\quad \left. + M_{y0}^2 \left(\frac{\partial^2 g_{1\infty}}{\partial \theta_y^2} \right)_{\theta_y=0} \right] \frac{1}{M_z^2} \frac{\omega^2 \tau}{1 + (\omega\tau)^2}. \end{aligned} \quad (\text{A7})$$

Now the Landau-Lifshitz equation of motion for the

¹⁹ A. M. Clogston, Bell System Tech. J. 34, 739 (1955).

magnetization is

$$d\mathbf{M}/dt = \gamma[\mathbf{M} \times \mathbf{H}] - (\lambda/M^2)[\mathbf{M} \times (\mathbf{M} \times \mathbf{H})]. \quad (\text{A8})$$

From this we calculate

$$dw/dt = \mathbf{H} \cdot d\mathbf{M}/dt = (\lambda/M^2)(\mathbf{M} \times \mathbf{H})^2, \\ \left\langle \frac{dw}{dt} \right\rangle_{\text{av}} = \frac{\lambda H^2}{2M^2}(M_{x0}^2 + M_{y0}^2). \quad (\text{A9})$$

H here is the total effective magnetic field as given by Eq. (1) in the text. If we use this relation, and set $\langle dw/dt \rangle_{\text{av}} = \langle dg/dt \rangle_{\text{av}}$, we find from Eqs. (A8) and (A9),

$$\lambda = \left[\left(\frac{\partial g_{100}}{\partial \theta_x^2} \right)_{\theta_x=0} + \frac{M_{y0}^2}{M_{x0}^2} \left(\frac{\partial g_{100}}{\partial \theta_y^2} \right)_{\theta_y=0} \right] \\ \times \frac{\gamma^2 \tau}{1 + (\omega\tau)^2} \frac{1}{1 + (M_{y0}^2/M_{x0}^2)}. \quad (\text{A10})$$

In our experiments most of the torque on the magnetization is due to the steady applied field, and is therefore circularly symmetrical about the z axis. Even the torque due to crystal anisotropy is circularly symmetrical in the $[100]$ and $[111]$ directions. We therefore assume that $M_{y0}^2 \cong M_{x0}^2$, and Eq. (A10) becomes

$$\lambda = \frac{1}{2} \left[\left(\frac{\partial^2 g_{100}}{\partial \theta_x^2} \right)_{\theta_x=0} + \left(\frac{\partial^2 g_{100}}{\partial \theta_y^2} \right)_{\theta_y=0} \right] \frac{\gamma^2 \tau}{1 + (\omega\tau)^2}. \quad (\text{A11})$$

Now by Eq. (9) in the text, we see that the width of the line at half-power points is $(2\Delta H)$:

$$2\Delta H = \frac{1}{M_z} \left[\left(\frac{\partial^2 g_{100}}{\partial \theta_x^2} \right)_{\theta_x=0} + \left(\frac{\partial^2 g_{100}}{\partial \theta_y^2} \right)_{\theta_y=0} \right] \frac{\omega\tau}{1 + (\omega\tau)^2}. \quad (\text{A12})$$

Magnetostriction and Permeability of Magnetite and Cobalt-Substituted Magnetite*

L. R. BICKFORD, JR.,† J. PAPPIS,‡ AND J. L. STULL

State University of New York, College of Ceramics, at Alfred University, Alfred, New York

(Received March 28, 1955)

The principal magnetostriction constants of magnetite were determined over the temperature range from 120°K to 300°K by the strain gauge technique. Since λ_{111} and λ_{100} are different in sign and practically constant over this entire range ($\lambda_{111} \approx +80 \times 10^{-6}$; $\lambda_{100} \approx -20 \times 10^{-6}$) the change in direction of easy magnetization which occurs at 130°K is manifested by a change in structure of λ vs H curves in a polycrystalline sample. The substitution of small amounts of cobalt for divalent iron in polycrystalline magnetite causes a marked shift upwards in the temperature of the maximum in initial permeability, which in the case of magnetite occurs at 130°K. The temperature shift is practically linear with respect to cobalt ferrite content, the rate being *ca* 140°C/mole percent. Magnetostriction vs magnetic field curves for these specimens indicate that the shifted permeability peak is still associated with a change in direction of easy magnetization. The predicted anisotropy of cobalt ferrite, obtained by extrapolation of these results, is in reasonable agreement with the values measured directly by other investigators.

I. INTRODUCTION

THIS paper concerns the magnetostriction and magnetocrystalline anisotropy of magnetite over a temperature range in which its symmetry is cubic (above 120°K). The anisotropy is a rapidly varying function of temperature in the vicinity of 130°K, at which temperature the direction of easy magnetization changes from $[111]$ to $[100]$.¹ The temperature spectrum of initial permeability in this region, shown

in Fig. 1, can be correlated directly with the absolute magnitude of the first-order anisotropy constant K_1 by the empirical relationship

$$\mu_0 - 1 = 39.1 M_s^2 / (|K_1| + 1.21 \times 10^4), \quad (1)$$

in which μ_0 is the absolute magnitude of the initial permeability, and M_s is the saturation magnetization (obtained from Pauthenet's data²). The constant term in the denominator is presumably associated with magnetostrictive strain energy.

Evidence that the magnetostriction varies widely in magnitude and even changes sign at low temperature has been reported.^{3,4} In order to check this temperature dependence directly, we have measured the principal

* This research was supported in part by the Office of Naval Research. Portions of this work were reported at two American Physical Society Meetings: Phys. Rev. **92**, 845(A) (1953); **94**, 1433(A) (1954).

† Now at International Business Machines Research Laboratories, Poughkeepsie, New York.

‡ Now at the Laboratory for Insulation Research, Massachusetts Institute of Technology, Cambridge, Massachusetts.

¹ L. R. Bickford, Jr., Phys. Rev. **78**, 449 (1950).

² R. Pauthenet, Ann. Physik **7**, 710 (1952).

³ C. A. Domenicali, Phys. Rev. **78**, 458 (1950).

⁴ J. L. Stull and L. R. Bickford, Jr., Phys. Rev. **92**, 845 (1953).